Journal of Pathology
J Pathol 2023
Published online 4 October 2023 in Wiley Online Library
(wileyonlinelibrary.com) DOI: 10.1002/path.6210

ORIGINAL ARTICLE

Genomic analysis of spermatocytic tumors demonstrates recurrent molecular alterations in cases with malignant clinical behavior

Sounak Gupta[1], Lynette M Sholl[2], Yiying Yang[3], Adeboye O Osunkoya[4], Jennifer B Gordetsky[5], Kristine M Cornejo[6], Kvetoslava Michalova[7], Fiona Maclean[8], Eugénia Dvindenko[9], Matija Snuderl[3], Michelle S Hirsch[2], William J Anderson[2], Ross A Rowsey[1], Rafael E Jimenez[1], John C Cheville[1], Peter M Sadow[6], Maurizio Colecchia[10], Costantino Ricci[11,12], Thomas M Ulbright[13], Daniel M Berney[14] and Andres Martin Acosta[2,13]*

[1] *Department of Pathology, Mayo Clinic, Rochester, MN, USA*
[2] *Department of Pathology, Brigham and Women's Hospital, Harvard Medical School, Boston, MA, USA*
[3] *Department of Pathology, New York University, New York, NY, USA*
[4] *Department of Pathology, Emory University School of Medicine, Atlanta, GA, USA*
[5] *Department of Pathology, Vanderbilt University, Nashville, TN, USA*
[6] *Department of Pathology, Massachusetts General Hospital, Harvard Medical School, Boston, MA, USA*
[7] *Department of Pathology, Charles University, Plzen, Czech Republic*
[8] *Department of Pathology, Douglass Hanly Moir Pathology, Macquarie University, Sydney, NSW, Australia*
[9] *Department of Pathology, Instituto Português de Oncologia, Lisbon, Portugal*
[10] *Department of Pathology, Universita Vita Salute San Raffaele, Milan, Italy*
[11] *Pathology Unit, Maggiore Hospital-AUSL Bologna, Bologna, Italy*
[12] *Department of Medical and Surgical Sciences (DIMEC), University of Bologna, Bologna, Italy*
[13] *Department of Pathology, Indiana University, Indianapolis, IN, USA*
[14] *Centre for Cancer Biomarkers & Biotherapeutics, Barts Cancer Institute, Queen Mary University of London, London, UK*

*Correspondence to: AM Acosta, Department of Pathology, Indiana University, 350 W. 11th Street, Room 4080, Indianapolis, IN 46202, USA.
E-mail: anmaacos@iu.edu

Abstract

Spermatocytic tumor (ST) is a rare type of germ cell tumor that occurs exclusively in the postpubertal testis and typically affects elderly men. Most STs are benign, but rare cases exhibit aggressive clinical behavior, often in association with transition to sarcomatoid histology. Limited molecular analyses have been performed on STs; therefore, their genomic and epigenomic features remain incompletely described. Twenty-seven samples from 25 individual patients were analyzed with a combination of DNA sequencing panels, genomic methylation profiling, SNP array, isochromosome (12p) [i(12p)] FISH, and immunohistochemistry. The series included five metastasizing tumors (three with sarcomatoid transformation, one anaplastic, and one conventional) and 20 non-metastasizing tumors (14 anaplastic and six conventional). Anaplastic tumors comprised a monomorphic population of intermediate-sized neoplastic cells, as previously described. Multiomic analyses demonstrated that there were two genomic subgroups of STs: one with diploid genomes and hotspot *RAS/RAF* variants and the other with global ploidy shift and absence of recurrent mutations. Relative gain of chromosome 9 was a consistent finding in both subgroups. A comparison of metastasizing and non-metastasizing cases demonstrated that aggressive behavior was associated with the acquisition of pathogenic *TP53* mutations and/or relative gains of 12p/i(12p). In cases with sarcomatoid transformation, *TP53* mutations seem to underlie the transition to sarcomatoid histology. Genomic methylation analysis demonstrated that aggressive cases with gains of 12p cluster closer to pure seminomas than to STs without gains of 12p. In conclusion, STs include two genomic subgroups, characterized by global ploidy shifts without recurrent mutations and diploid genomes with *RAS/RAF* hotspot mutations, respectively. Biologic progression was associated with relative gains of 12p and *TP53* mutations. The findings in STs with relative gains of 12p suggest that they may exhibit biologic characteristics akin to those seen in germ cell neoplasia *in situ*-related germ cell tumors rather than non-germ cell neoplasia *in situ*-derived STs.

Keywords: testis; spermatocytic tumor; germ cell tumor; GCNIS; i(12p); testicular cancer; genomic analysis; non-GCNIS-derived germ cell tumor

Received 12 June 2023; Revised 3 August 2023; Accepted 24 August 2023

No conflicts of interest were declared.

Introduction

Spermatocytic tumor (ST) is a rare type of testicular germ cell tumor that affects post-pubertal patients and is considered unrelated to germ cell neoplasia *in situ* (GCNIS) [1–3]. As its name implies, ST is thought to derive from adult spermatogonial cell populations and recapitulate stages of spermatocyte maturation.

Typical cases exhibit a triphasic morphology characterized by the presence of small, intermediate, and large neoplastic germ cells. A smaller subset of ST, often referred to as 'anaplastic', is rather monomorphic, with a uniform population of intermediate-sized cells in contrast to its more conventional counterpart [4,5]. The vast majority of STs are benign and can therefore be managed conservatively after radical orchiectomy [3]. However, rare cases may undergo sarcomatoid transformation and behave in a malignant manner [6–8]. Malignant behavior may also be seen in extremely rare STs with anaplastic or conventional histology [3,9].

Few STs have been analyzed using molecular profiling techniques. Based on the limited number of STs assessed thus far, genome doubling events with superimposed recurrent chromosomal gains and losses (that result in dysregulation of genes that control the mitotic-to-meiotic transition) are hypothesized to represent an oncogenic mechanism in these tumors [2]. Additionally, mutations of MAPK pathway genes are also a recurrent finding and probably play a relevant biologic role in a subset of STs [2].

Of note, findings consistent with isochromosome 12p [i(12p)], which are thought to be restricted to GCNIS-derived tumors, have been identified in rare cases of STs with anaplastic morphology and/or aggressive clinicopathologic features. Therefore, some studies have suggested that the over-representation of sequences present in the short arm of chromosome 12 may be associated with distinct biologic and phenotypic characteristics in this tumor type [2,4,5]. However, these data come from reports of relatively small numbers of cases with limited molecular analyses (largely SNP array and FISH). Hence, the genomic alterations associated with malignant behavior in ST remain incompletely understood. In this study, we performed multiomic characterization of clinically malignant and benign STs, including cases with conventional, anaplastic, and sarcomatoid histology, using large panel next generation sequencing (NGS) assays, SNP array, i(12p) FISH, and genome-wide methylation profiling.

Materials and methods

Patient specimens

This research was performed with the approval of the institutional review board of Brigham and Women's Hospital (MGB Insight 4.0, protocol #2021P002289), Mayo Clinic (protocol #19-010758), and the remaining participating institutions (when applicable). Informed consent was waived.

The pathology archives of the participating institutions and personal consultation files of the authors were queried to identify STs with conventional, anaplastic, and sarcomatoid histology. Cases were considered anaplastic if they predominantly consisted of a uniform population of intermediate-sized neoplastic cells (unlike the typical triphasic morphology seen in conventional STs). This series was intentionally enriched for anaplastic STs and STs with sarcomatoid transformation, with selected conventional STs included for comparison.

Candidate cases with archival FFPE tissue were re-reviewed at the participating institutions by dedicated genitourinary pathologists. Subsequently, selected slides of qualifying cases were centrally reviewed by two authors (SG and AMA).

Tissue macrodissection for nucleic acid extraction

Consecutive FFPE tissue sections (5 μm) were obtained from the blocks of interest and the first section was stained with H&E. The H&E slides were assessed and annotated by a genitourinary pathologist (SG or AMA) to guide manual dissection of the corresponding unstained FFPE tissue sections. More specifically, tumor areas were marked and dissected away from the surrounding non-neoplastic tissue. In two sarcomatoid STs (cases 1 and 2) with material from both histologic components (conventional and sarcomatous) available for the study, these were dissected from separate blocks containing exclusively the component of interest to avoid cross-contamination.

DNA sequencing

Molecular profiling was performed using two separate NGS assays, both of which required manual macrodissection for tumor enrichment prior to extraction of genomic DNA (as described above). The first assay, Oncopanel ($n = 18$), was performed as previously reported in validation studies [10,11]. The current version of this solid tumor panel covers the coding sequencing of 447 cancer-relevant genes (listed in supplementary material, Appendix S1). This tumor-only assay uses a clinically validated informatics pipeline for the detection of SNV/indels, copy number changes, and structural variants [12]. Mismatch repair status and mutational signatures are also evaluated using in-house algorithms [13,14]. In this assay, variants reported at frequencies >0.1% in gnomAD are automatically filtered out to avoid including germline events. All annotated variants were further evaluated for clinical significance, biologic relevance, and actionability by a molecular pathologist (LMS). A second clinically validated assay, MayoComplete solid tumor panel, was performed on a subset of samples ($n = 4$) to interrogate the coding sequence of 515 genes (listed in supplementary material Appendix S2) for SNVs/indels. This assay is also clinically validated to evaluate tumor mutation burden, microsatellite instability, and the amplification status of 59 genes, while copy number changes for other target genes can be assessed for investigational purposes. This test was not designed to distinguish between somatic and germline alterations [15,16]. All annotated variants were further evaluated for clinical significance, biologic relevance, and actionability by a molecular pathologist (SG).

LOH was assessed at the individual gene level for variants of interest and across chromosomal regions. More specifically, LOH for individual genes was inferred when there were two or more concurrent pathogenic events occurring in trans (e.g. two or more pathogenic SNVs, one pathogenic SNV with copy number loss of the wild-type allelle). LOH across genomic regions was determined by evaluating imbalances of SNPs (i.e. ratio of major-to-minor allele) with OncoPanel [10,11].

SNP array

The OncoScan® FFPE Assay Kit (Thermo Fisher Scientific, Santa Clara, CA, USA) was used to evaluate isolated DNA. The technical details of the molecular inversion probe method have been described previously [5,17–19]. In brief, a molecular inversion probe targeting a unique SNP or base pair of interest anneals to isolated DNA and circularizes with its complementary nucleotides. A gap-filling step closes the circularized DNA and single-stranded material is destroyed. The circular probe is then released, cleaved, becomes inverted, and is amplified using universal primers. The biotinylated oligonucleotides are then hybridized overnight to a microarray. Data files were analyzed using Affymetrix ChAS software (Thermo Fisher Scientific).

Fluorescence *in situ* hybridization

FISH for i(12p) was performed as described previously [18]. Laboratory-developed *PKP2/D12Z3* probe sets consisting of *PKP2* DNA (Mayo LDT, clones: RP11-8P13, RP11-267D19, and RP11-855O3) labeled with SpectrumOrange (red, 'R') and *D12Z3/CEN12* DNA probes (Abbott Molecular/Vysis, Abbott Park, IL, USA) labeled with SpectrumGreen (green, 'G') were applied to individual slides, hybridized, and washed according to the PAT Reduced Pepsin FISH protocol. The centromeric probe (G) and the locus-specific probe for the *PKP2* gene region (R) exhibiting a 1R1G1R signal pattern was interpreted as an i(12p) signal. Two technologists independently scored 50 qualifying representative tumor nuclei from areas specified by a pathologist. Tumor samples were interpreted as positive for i(12p), if the corresponding signal (1R1G1R) was present in more than 30% of the cells analyzed [18].

Genomic methylation analysis

Genomic methylation profiling was performed as described previously [20]. In brief, FFPE tissue was macrodissected to optimize tumor content for DNA extraction. The DNA was processed for hybridization and fluorescence staining on the Infinium MethylationEPIC (850 k) BeadChip array (Illumina, San Diego, CA, USA) following the manufacturer's recommendations. Arrays were scanned in an Illumina iScan microarray scanner (Illumina), and the raw idat files were analyzed in R (R Foundation for Statistical Computing, Vienna, Austria). Raw intensities were processed with Bioconductor R package Minfi [21] and each sample was assessed for quality by mean detection p value ($p < 0.05$). Each sample was normalized by quantile normalization, followed by removal of probes that failed in one or more samples (detection $p < 0.01$) or that contained SNPs. β values were calculated with the default offset value 100, as recommended for Illumina assays. Methylation profiles of STs (conventional, $n = 4$; anaplastic, $n = 10$; sarcomatoid, $n = 1$) and pure classic-type seminomas ($n = 3$) were compared. After fitting linear models with limma (3.48.3) (https://bioconductor.org/packages/release/bioc/html/limma.html), top differentially methylated probes were selected based on adjusted p values ($p < 0.05$). Hypomethylation was defined as a β value < 0.2, whereas hypermethylation was defined as a β value > 0.8. A heatmap was generated by ComplexHeatmap (2.8.0) based on the hierarchical clustering of the top 1,000 differentially methylated probes [22].

Immunohistochemistry

Immunohistochemistry was performed at Brigham and Women's Hospital, Mayo Clinic, and Indiana University following validated institutional protocols with the following primary antibodies: SALL4 (clone 6E3, Abnova, Taipei, Taiwan; clone 6E3, Cell Marque, Rocklin, CA, USA; RTU/prediluted and dilution 1:600, respectively), OCT3-4 (clone N1NK, Dako, Carpinteria, CA, USA; clone N1NK, Leica Biosystems, Deer Park, IL, USA; dilution 1:50), SSX (clone E5A2C, Cell Signaling, Danvers, MA, USA; dilution 1:800), p53 (clone DO-7, Dako; dilution 1:400), and NRASQ61R (clone SP174, Abcam, Cambridge, MA, USA; dilution 1:50).

Results

Clinicopathologic characteristics of the series

The study comprised 25 STs (27 samples) from 25 individual patients with a median age of 53 years (range: 30–83 years). Nine cases had been previously reported in four separate studies (cases 1, 3–6, and 19–22) [5,6,8,9]. Five patients (cases 1–5) presented with metastatic disease or developed metastases during follow-up (Table 1). The remaining 20 patients had no evidence of metastases after follow-up periods that ranged from 0 to 258 months (median: 27.5 months).

Four cases exhibited sarcomatoid transformation (cases 1–3 and 6; Figure 1A–D), 15 cases had so-called anaplastic features (cases 5, 8–12, 14, 16–18, and 21–25; Figure 2A), and the remaining six cases had conventional morphology (Figure 2B). Tumors with sarcomatoid transformation were characterized by the presence of histologic components of rhabdomyosarcoma (case 2), high-grade unclassified/pleomorphic sarcoma (cases 1, 3, and 6), and chondrosarcoma (case 6). The transition from conventional to sarcomatoid histology was abrupt and, in cases with biopsy-proven metastases, only the sarcoma components were present at metastatic

Table 1. Clinicopathologic features of 25 patients with STs.

Case	Age	Histology	Metastasis	Metastatic sites	Adverse features†	Follow-up (months)‡
1*	46	Sarcomatoid	Metastasizing	Lung	Not applicable	15 months – AWD (widely metastatic)
2	55	Sarcomatoid	Metastasizing	Lung and multiple lymph nodes (supraclavicular, paratracheal, hilar, para-aortic, inguinal)	Not applicable	3 months – died of complications related to treatment
3*	63	Sarcomatoid	Metastasizing	Lung	Not applicable	Not available/0
4*	30	NOS/conventional	Metastasizing	Lung	Not applicable	72 – NED
5*	42	Anaplastic	Metastasizing	Retroperitoneal lymph nodes	Present (locally aggressive, LVI)	13 – AWD
6*	52	Sarcomatoid	Non-metastasizing	Not applicable	Present (LVI)	Not available/0
7	39	NOS/conventional with GCNIS	Non-metastasizing	Not applicable	Not applicable	72
8	43	Anaplastic	Non-metastasizing	Not applicable	Not identified	Not available/0
9	51	Anaplastic	Non-metastasizing	Not applicable	Not identified	Not available/0
10	71	Anaplastic	Non-metastasizing	Not applicable	Not identified	76
11	83	Anaplastic	Non-metastasizing	Not applicable	Not identified	25
12	58	Anaplastic	Non-metastasizing	Not applicable	Not identified	258
13	53	NOS/conventional	Non-metastasizing	Not applicable	Not identified	1
14	62	Anaplastic	Non-metastasizing	Not applicable	Not identified	94
15	54	NOS/conventional	Non-metastasizing	Not applicable	Present (LVI)	38
16	61	Anaplastic	Non-metastasizing	Not applicable	Not identified	Not available/0
17	32	Anaplastic	Non-metastasizing	Not applicable	Not identified	19
18	67	Anaplastic	Non-metastasizing	Not applicable	Not identified	Not available/0
19*	71	NOS/conventional	Non-metastasizing	Not applicable	Not identified	94
20*	43	NOS/conventional	Non-metastasizing	Not applicable	Not identified	Not available/0
21*	43	Anaplastic	Non-metastasizing	Not applicable	Not identified	Not available/0
22*	40	Anaplastic	Non-metastasizing	Not applicable	Present (LVI)	Not available/0
23	62	Anaplastic	Non-metastasizing	Not applicable	Present (LVI)	121
24	39	Anaplastic	Non-metastasizing	Not applicable	Not identified	30
25	69	Anaplastic	Non-metastasizing	Not applicable	Not identified	14

AWD, alive with disease; LVI, lymphovascular invasion; NED, no evidence of disease; NOS, not otherwise specified.
*Cases previously reported (see references [5,6,8,9]).
†Presence of adverse histopathologic findings in primary tumors (i.e. orchiectomies) of patients without known metastatic disease.
‡For non-metastasizing cases.

sites. In two cases with sarcomatoid transformation (cases 3 and 6), the non-sarcomatoid component had a monomorphic (i.e. anaplastic) appearance. Tumors with conventional morphology frequently exhibited abundant mitoses, karyorrhexis, scattered large nuclei with filamentous ('spireme') chromatin, as well as intratubular patterns of growth.

The only tumor with sarcomatoid histology and no evidence of metastases (case 6) exhibited overt lymphovascular invasion (conventional ST component) in the orchiectomy specimen. Of note, follow-up was not available for this patient. Among the remaining non-metastasizing cases (cases 7–25), lymphovascular invasion was seen in three cases (cases 15 and 22–23), including a patient with bilateral STs (case 23). Case 7 was unique in that it consisted of an otherwise typical ST adjacent to foci of GCNIS (supplementary material, Figure S1). In this case, OCT4 immunohistochemistry highlighted the GCNIS and was entirely negative in the ST. The presence of concurrent GCNIS and ST can be considered an exceptional occurrence, and it is uncertain if it represents a causal or a random association. All neoplasms with 'anaplastic' features lacked expression of immunomarkers typically expressed by seminoma (OCT3/4, PLAP).

Molecular analyses

In total, 27 samples from 25 individual patients were analyzed using DNA sequencing, SNP array, i(12p) FISH, immunohistochemistry, or a combination thereof. These samples included paired sarcomatoid and conventional histologic components of cases 1 and 2 (four samples), and whole tumor tissue of cases 3–25 (23 samples). Cases were worked up as follows: (1) i(12p) FISH only: three cases (cases 23–25), (2) DNA sequencing only: 12 cases (cases 1 and 8–18), (3) DNA sequencing and i(12p) FISH: two cases (cases 3 and 6), (4) DNA sequencing and SNP array: six cases (cases 2, 4, 7, 19–21), and (5) DNA sequencing, SNP array, and i(12p) FISH: two cases (cases 5 and 22). The work-up performed on each sample is detailed in Figure 3A.

DNA sequencing results

Overall, DNA sequencing was attempted on 22 cases (cases 1–22), including paired analysis of sarcomatoid and conventional ST components of cases 1 and 2. Nineteen cases underwent successful sequencing, whereas three failed standard quality assurance metrics (cases 8 and 15–16).

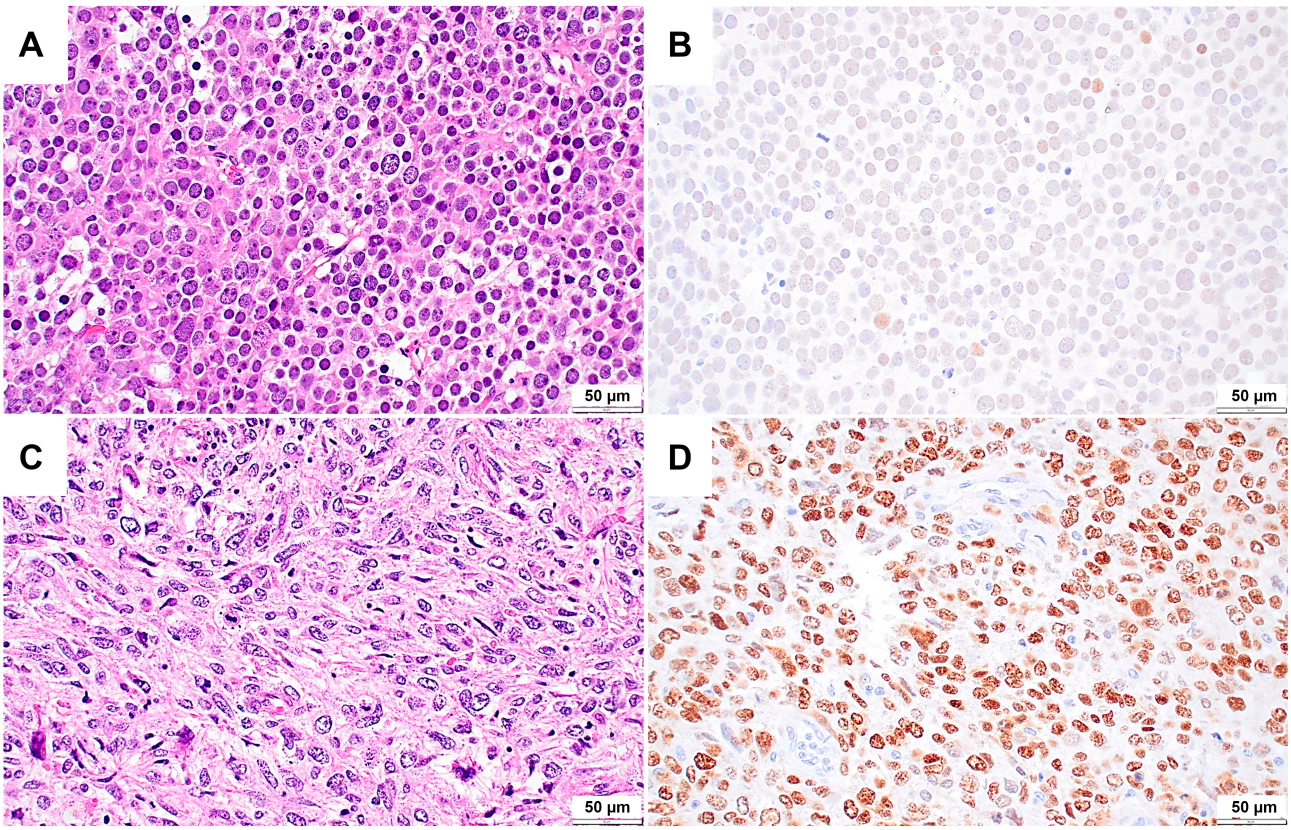

Figure 1. ST with sarcomatoid transformation. (A) Conventional component of case 1. (C) The sarcomatoid component of case 1 consisted of a high-grade unclassified sarcoma. The pattern of expression of p53 was heterogeneous (i.e. 'wild-type') in the conventional histologic component (B), and overexpressed (i.e. mutant pattern) in the sarcomatoid component (D).

Analyses of SNVs demonstrated the presence of hotspot pathogenic mutations in MAPK pathway GTPases in 6/19 (~32%) cases sequenced successfully, including *NRAS* (4/6), *HRAS* (1/6), and *BRAF* (1/6) variants (Table 2, Figure 3A). Pathogenic *TP53* variants were present in all cases with sarcomatoid histology (4/4, cases 1–3 and 6). Analysis of paired sarcomatoid and conventional components in case 1 demonstrated that the *TP53* variant was present only in the sarcomatoid component. Similarly, in case 2, a pathogenic *TP53* variant was present in the sarcomatoid component, with molecular evidence of LOH. The conventional component of this tumor also harbored a *TP53* variant of uncertain significance (p.P12R). In the two remaining sarcomatoid neoplasms (cases 3 and 6) the different histologic components were not analyzed individually, but immunohistochemistry results were consistent with a mutant pattern of

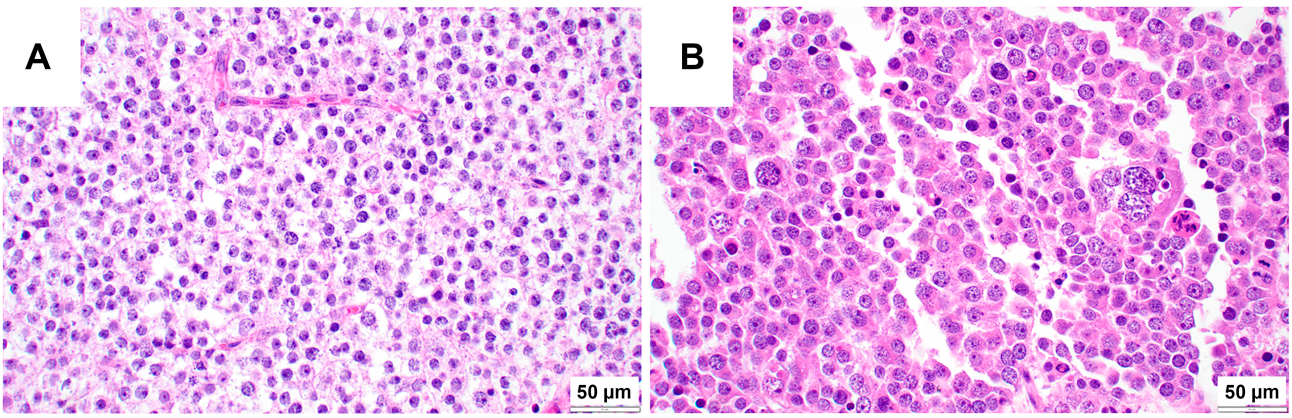

Figure 2. Anaplastic and conventional STs. (A) Case 11 comprised a homogeneous population of intermediate-sized neoplastic cells, consistent with so-called 'anaplastic' ST. (B) Case 15 exhibited the typical triphasic histology, with large, intermediate-sized and small neoplastic cells with abundant apoptotic bodies. Scattered large cells contain filamentous ('spireme') chromatin.

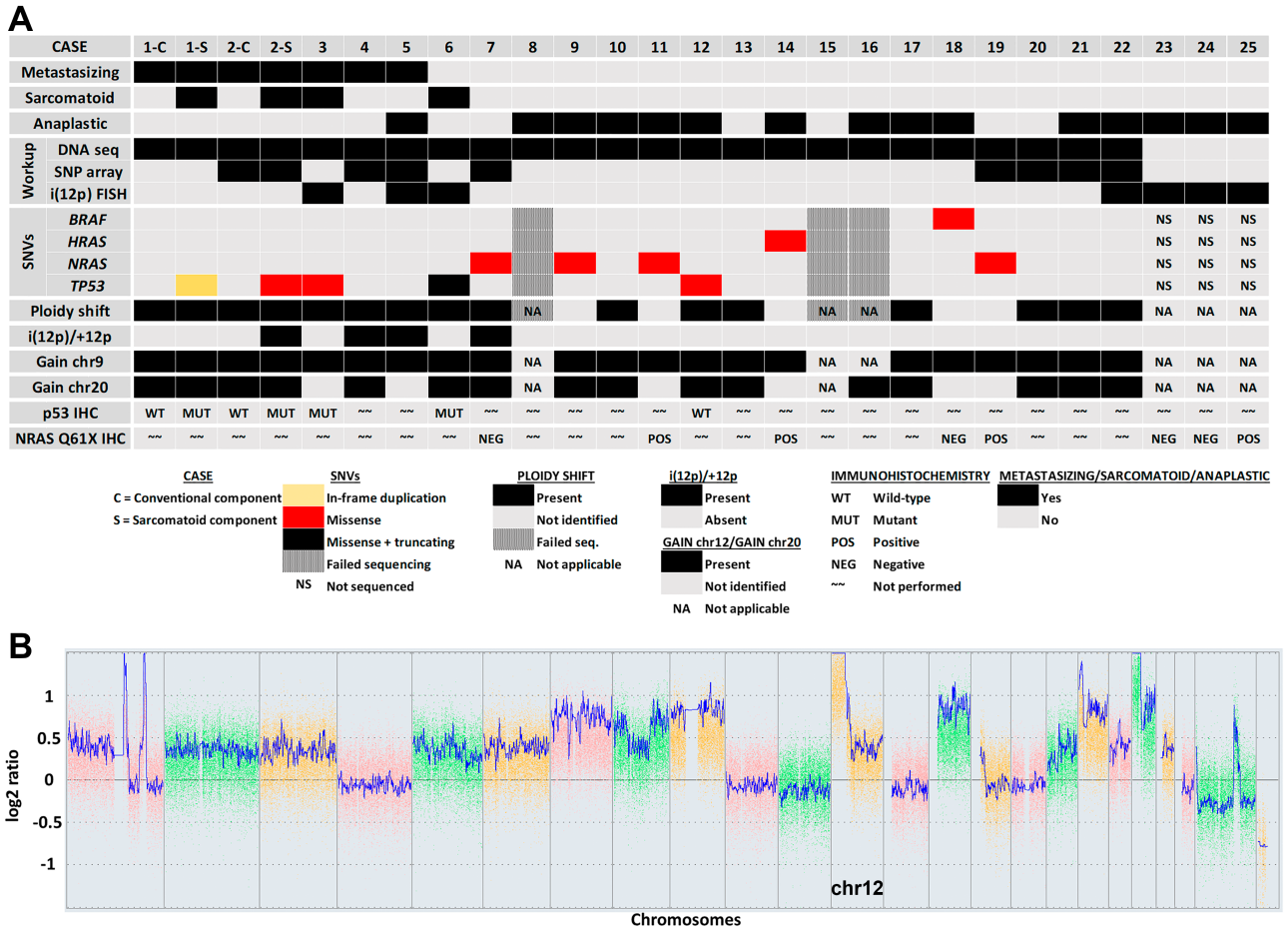

Figure 3. Molecular findings in STs. (A) Summarized results of molecular and immunohistochemical analyses of STs from 25 patients. In cases 1 and 2, the conventional ('C') and sarcomatoid ('S') components were individualized and sequenced in parallel. For p53 immunohistochemistry, 'wild-type' and 'mutant' expression patterns denote nuclear expression in scattered neoplastic nuclei and diffuse expression in >75% of neoplastic nuclei (or complete loss of expression), respectively. (B) SNP array analysis of case 4 demonstrates findings consistent with i(12p). chr, chromosome; IHC, immunohistochemistry.

expression only in the sarcomatoid components (see immunohistochemistry results below). Non-recurrent variants of uncertain biologic significance were also identified in individual cases (Table 2).

Evidence of a global shift in ploidy (≥49 autosomes), ranging from hyper-diploid to near-tetraploid genomes, was identified in 14 of 19 cases that were sequenced successfully (~74%), whereas the remaining five (~26%) appeared to be diploid with focal copy number changes. All cases with seemingly diploid genomes (cases 9, 11, 14, and 18–19) harbored hotspot SNVs in MAPK pathway GTPases. In contrast, only one case with global ploidy shift had a concurrent GTPase (*NRAS*) mutation (case 7). Relative copy number gains involving the entirety or large regions of chromosome 9 were identified in all cases that were sequenced successfully (19/19, 100%). In other words, the estimated copy number status of chromosome 9 was above the estimated baseline ploidy of each individual case (e.g. four or more copies in a case with a triploid baseline). Similarly, relative gains of chromosome 20 were identified in 13/19 cases (~68%) sequenced successfully. A relative loss of chromosome 7 was identified in 3/19 cases (~16%). Relative gains of 12p were detected in 4/19 cases (~21%; sarcomatoid component of cases 2 and 4, anaplastic ST case 5, and conventional ST case 7). Focal amplification events were identified in four cases, all metastasizing (cases 1–3 and 5). In cases 1 and 2, the amplifications were identified only in the sarcomatoid components of the tumors. The genes involved in the amplification events included (but were not restricted to): *PDGFRA* (case 1), *KIT* (case 1), *MPL* (case 2), *MYCL* (case 2), *MCL1* (case 2), *FGFR1* (case 3), and *KRAS* (case 5).

In summary, four of the five cases with *TP53* mutations were sarcomatoid (80%, cases 1–3 and 6) and the remaining one was anaplastic (case 12). Four of the five cases with seemingly diploid genomes and hotspot MAPK GTPase mutations were anaplastic (80%, cases 9, 11, 14, and 18) and the remaining one exhibited conventional histologic features (case 19). Three of the four cases with relative gains of 12p were metastasizing (sarcomatoid component of case 2 and cases 4–5), whereas the remaining one was non-metastasizing (case 7). The histology of cases with relative +12p spanned the whole morphologic spectrum represented in this

Table 2. SNVs in 22 STs analyzed with NGS.

Case	Sample	SNV/indels (VAF)
1	Sarcomatoid (sarcomatoid component)	*TP53* p.N235_Y236dup (67%)
	Sarcomatoid (conventional component)	None identified
2	Sarcomatoid (sarcomatoid component)	*TP53* p.R273C (67%, and LOH)
	Sarcomatoid (conventional component)	*TP53* p.P12R (69%, likely VUS)
3	Sarcomatoid	*TP53* p.R273C (70%)
4	NOS/conventional	None identified
5	Anaplastic	None identified
6	Sarcomatoid	*TP53* p.R342* (13%), *TP53* p.R273H (50%), *RAC1* p.A159V (35%)
7	NOS/conventional	*NRAS* p.G12A (48%)
8	Anaplastic	Cannot be determined
9	Anaplastic	*NRAS* p.Q61R (45%)
10	Anaplastic	None identified
11	Anaplastic	*NRAS* p.Q61R (30%)
12	Anaplastic	*TP53* p.Y205S (55%), *TP53* p.R267W (26%)
13	NOS/conventional	None identified
14	Anaplastic	*HRAS* p.Q61R (84%)
15	NOS/conventional	Cannot be determined
16	Anaplastic	Cannot be determined
17	Anaplastic	None identified
18	Anaplastic	*BRAF* p.K601E (21%), *BRAF* p.S614C (18%), *ERCC3* p.Q373_W374ins* (52%, no LOH)
19	NOS/conventional	*NRAS* p.Q61R (36%), *NOTCH3* p.R103* (51%, no LOH)
20	NOS/conventional	None identified
21	Anaplastic	None identified
22	Anaplastic	*KDM6A* p.V1356Kfs21* (36%, no LOH)

NOS, not otherwise specified; VAF, variant allele frequency; VUS, variant of uncertain significance.

series, from conventional (cases 4 and 7), to anaplastic (case 5), and sarcomatoid (case 2).

SNP array and i(12p) FISH results

SNP array and/or FISH studies were performed to further investigate the presence of i(12p)/relative gains of 12p in a selected subset of cases ($n = 13$). This included: (1) four cases with evidence of +12p on DNA sequencing (three metastasizing: cases 2 and 4–5; one non-metastasizing: case 7), (2) two metastasizing and four non-metastasizing cases without evidence of +12p on DNA sequencing (two conventional: cases 19–20; two anaplastic: cases 21–22), and (3) and three non-metastasizing cases with anaplastic histology and no DNA sequencing data (i.e. unknown copy number status; cases 23–25). In case 2, SNP array was performed on paired sarcomatoid and conventional histologic components, demonstrating relative gains of 12p only in the former. Overall, findings consistent with i(12p) or +12p by SNP array and/or FISH were identified in four cases (sarcomatoid component of case 2, anaplastic ST case 5, and conventional ST cases 4 and 7; Figure 3B and supplementary material, Figure S2), whereas the remaining samples ($n = 9$) were negative. In the case in which i(12p) was identified by FISH (case 5), multiple copies of the isochromosome were present in 74% of the tumor nuclei, comparable to the values often seen in seminoma.

Genome methylation analysis

Methylation profiling was performed on 16 samples from 15 cases with additional material available, including two metastasizing cases (cases 2 and 5) and 13 non-metastasizing cases (nine anaplastic: cases 10–12, 14, 16–18, and 21–22; four conventional: cases 13, 15, 19, and 20). The conventional and sarcomatoid histologic components of case 2 were independently profiled. Three pure seminomas with typical histologic features were analyzed for comparison. Unsupervised clustering using the top 1,000 differentially methylated probes demonstrated that both case 5 and the sarcomatoid component of case 2 clustered closer to the three seminomas (Figure 4). In contrast, the conventional component of case 2 as well as the remaining STs clustered separately. Of note, both the sarcomatoid component of case 2 and case 5 harbored relative gains of 12p. Interestingly, cases with GTPase mutations also demonstrated a tendency to cluster together.

Immunohistochemistry

Immunohistochemistry for p53 and NRAS/HRAS protein with codon 61 mutations (mutation-specific NRAS/HRASQ61X) was performed on selected cases with additional material available and pathogenic variants in these genes detected by DNA sequencing. Moreover, NRAS/HRASQ61X was also performed in the three cases of the series without prior genomic characterization (cases 23–25).

Immunohistochemistry demonstrated that all sarcomatoid cases with *TP53* mutations (cases 1–3 and 6) overexpressed p53 (i.e. mutant pattern; Figure 1); in contrast, case 12 showed a 'wild-type' (i.e. heterogeneous) pattern of expression, that was discordant with sequencing results (p.Y205S and p.R267W). In all sarcomatoid STs, overexpression of p53 was restricted to the sarcomatoid components, with 'wild-type' expression in the non-sarcomatoid histologic elements. Mutation-specific NRAS/HRAS immunohistochemistry was positive in all tested cases with known *NRAS* or *HRAS* codon 61 variants (cases 11, 14, and 19) and in one case without genomic characterization (case 25). In all of them, strong and diffuse positivity was observed, with expression of the mutant form of the protein in virtually every neoplastic cell. This finding suggests that the GTPase variants present in these

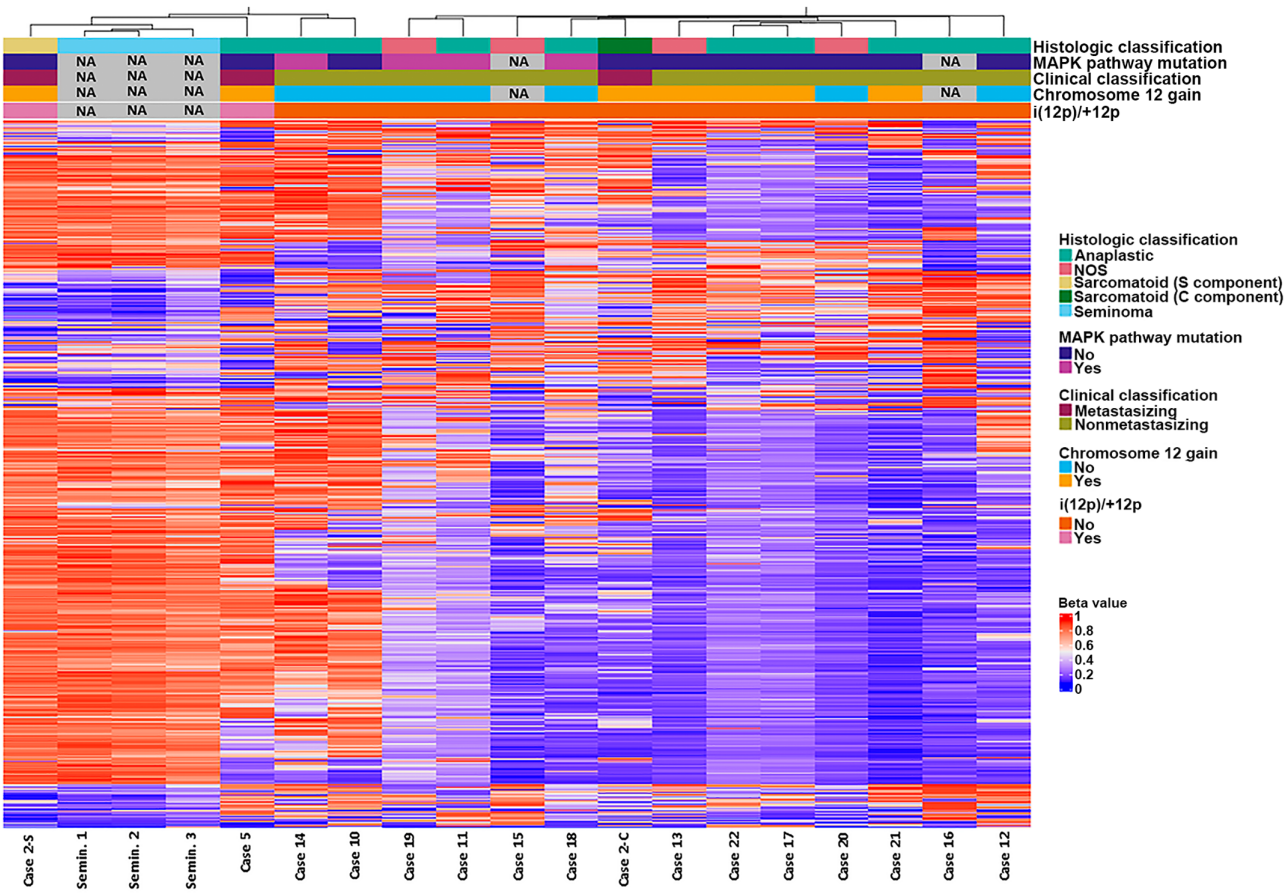

Figure 4. Genomic methylation profiling of STs and pure seminomas. Unsupervised clustering based on the top 1,000 differentially methylated probes demonstrates that two clinically malignant tumors (the sarcomatoid component of case 2 and case 5) cluster closer to seminomas than to the remaining STs (all clinically indolent). NA, not applicable; NOS, conventional/not otherwise specified; Semin., seminoma. MAPK pathway mutations denotes the presence of hotspot variants in GTPase genes of the MAPK pathway (NRAS, HRAS, or BRAF). In the key, 'C' and 'S' denote the conventional and sarcomatoid components of case 2, respectively.

cases probably represent clonal events with a purported driver role.

Discussion

Unlike GCNIS-related germ cell tumors (also referred to as type II germ cell tumors), which arise as a consequence of genetic reprogramming of early germ cell precursors, STs are thought to represent neoplastic transformation of more mature germ cell progenitors and are not associated with GCNIS [1,2]. From a developmental perspective, STs are considered type III tumors and do not have ovarian or extragonadal counterparts [1]. Based on data from prior studies, STs exhibit distinct pathologic, pathogenetic, and genomic characteristics that do not seem to overlap significantly with those of other germ cell tumor types. Although the vast majority of STs are benign and therefore cured by radical orchiectomy, rare cases may undergo sarcomatoid transformation and follow an aggressive clinical course [6–8].

Prior genomic analyses demonstrated that STs have a low mutational burden and a subset harbors hotspot mutations in GTPase or protein kinase genes that are hypothesized to confer a growth advantage that leads to clonal expansion of the mutant spermatogonia, creating a window of opportunity for additional oncogenic events to accumulate, ultimately resulting in the development of STs [2,23]. Thus far, activating *FGFR3*, *NRAS*, and *HRAS* mutations have been described in STs, and tumors with GTPase or kinase mutations often occur in older patients when compared with STs without these alterations [2]. The mutational patterns of STs are characterized by a predominance of C > T transitions in the context of ACG sequences (ACG > ATG), which occur as a consequence of deamination of 5-methylcytosine [2]. This contrasts with the predominant mutational pattern seen in *de novo* germline mutations, which are enriched in C > T transitions seen in the context of CCG sequences (CCG > CTG) [24].

STs are typically aneuploid, with genomes that vary from near-diploid to near-tetraploid (median number of autosomes: 72; range 50–99) [2,25–27]. Moreover, these neoplasms harbor recurrent chromosomal gains and losses relative to their basic ploidy, including +9, +20, −7, −13, −15, and −22 [2]. Relative gains of chromosome 9 are almost invariably seen in STs, with *DMRT1* (located in 9p21.3-pter) being identified as the most likely candidate gene relevant for oncogenesis [26]. *DMRT1* and *SOHLH1*, another gene located in chromosome 9, are

important coordinators of the progression from mitosis to meiosis, which marks the transition from spermatogonia to spermatocytes, and play a role in maintenance of the spermatogonial stem cell pool [28]. More specifically, down-regulation of *DMRT1* and *SOHLH1* is required to release their inhibitory effect on *STRA8*, a retinoic acid-response gene located on chromosome 7 that promotes progression to meiosis [29]. It has been hypothesized that the relative gains of chromosome 9 (*DMRT1*, *SOHLH1*) and loss of chromosome 7 (*STRA8*) in STs lead to imbalances in the expression of the respective protein products, preventing the neoplastic spermatogonia from entering meiosis, although some cells may escape this mechanism and enter a meiotic program [2]. This would explain the heterogeneous cell population and DNA content typically seen in STs.

Like seminomas, STs are characterized by globally hypomethylated genomes. However, a key difference between these tumor types is that seminomas exhibit a somatic imprinting profile, consistent with their origin from an early germ cell precursor that predates the erasure of imprinting patterns [30]. In contrast, STs exhibit a paternal imprinting pattern, suggesting that they derive from a more mature precursor (possibly in a late spermatogonial or spermatocytic stage) [30]. Conventional (i.e. typical) STs demonstrate markedly heterogeneous intratumoral morphologic features, which is paralleled by a significant degree of epigenomic heterogeneity [31]. More specifically, STs contain subpopulations of neoplastic cells with different patterns of histone methylation and expression of methyltransferases, which do not show a clear correlation with cell size [31]. Whether this 'epigenomic' instability is also a feature of tumors with more uniform histologic features (e.g. 'anaplastic' STs) is currently uncertain.

A subset of STs composed of a uniform population of intermediate-sized neoplastic cells (anaplastic ST) and those exhibiting sarcomatoid transformation have been associated with a higher incidence of malignant behavior than STs with conventional morphology [3]. So-called anaplastic STs demonstrate significant morphologic overlap with seminoma but lack expression of transcription factors associated with a primitive (pluripotential) germ cell state (such as OCT3/4 and NANOG) and are unassociated with GCNIS [4,18]. Studies of anaplastic STs have demonstrated that those with aggressive clinicopathologic features may harbor relative gains of 12p such as i(12p) [4,5]. In these cases, gains of 12p seem to be present with concurrent gains of chromosome 9 that encompass the *DMRT1* locus. An aggressive case with conventional histology and evidence of i(12p) has also been documented (included as case 4 in this study) [9]. However, the molecular

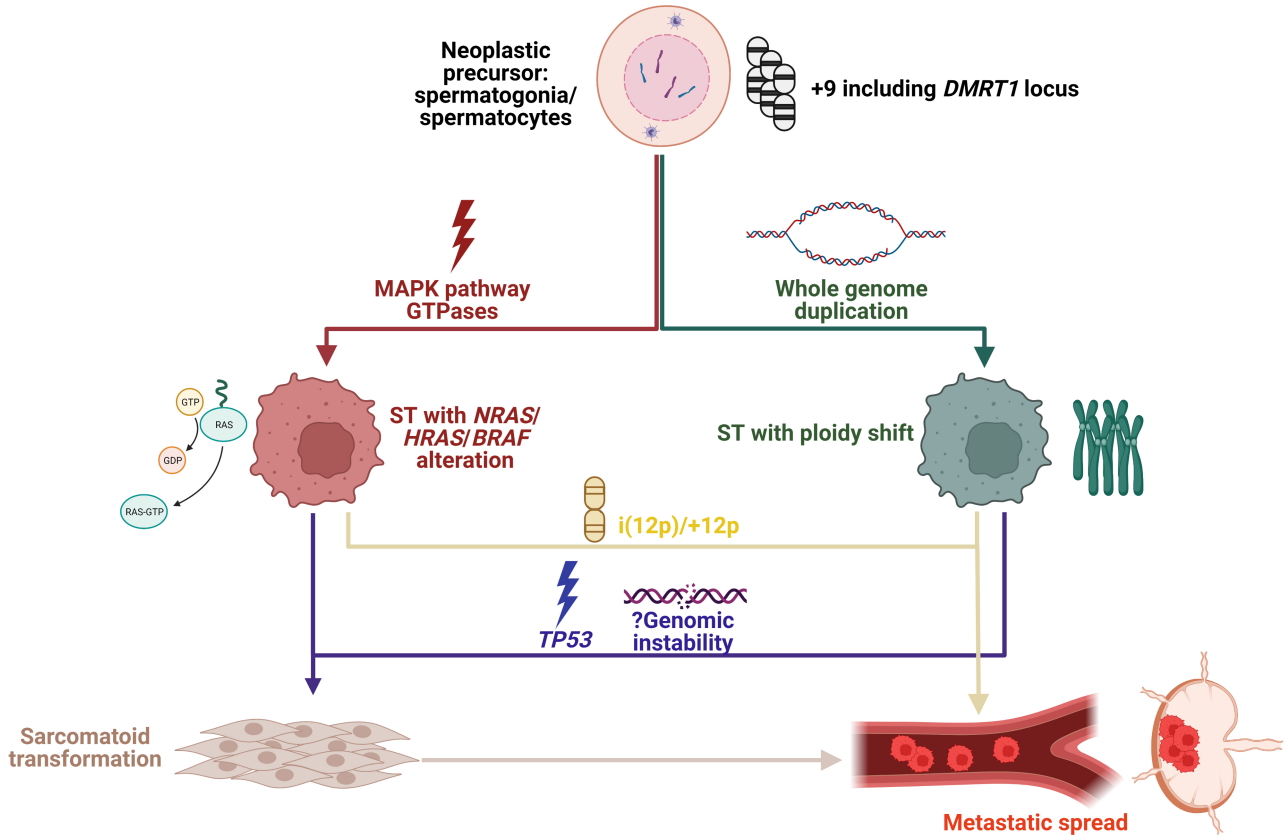

Figure 5. Genomic subtypes and hypothetical mechanisms of progression of STs. Although no case with *NRAS/HRAS/BRAF* alteration was metastatic in this study, given the limited number of malignant tumors analayzed and the co-occurrence of a hotspot *NRAS* mutation and i(12p) in case 7, the hypothetical possibility of gains of 12p leading to progression in tumors with mutations of MAPK pathway GTPases is depicted. Figure created with BioRender.com.

alterations associated with sarcomatoid transformation had not been described previously. The results of the present study suggest that aggressive clinical behavior in STs is associated with relative gains of 12p and/or pathogenic alterations of p53. The former was found in aggressive cases with conventional (case 4), anaplastic (case 5), and sarcomatoid (case 2) features. In case 2, the relative gain of 12p was identified only in the sarcomatoid component of the tumor. In all of them, concurrent relative gains (i.e. above the baseline ploidy) of chromosome 9 were also present. Transition to sarcomatoid histology in STs seems to be consistently associated with the acquisition of pathogenic *TP53* variants. Only one case with pathogenic *TP53* variants (case 12) demonstrated indolent clinical behavior after a long follow-up period (258 months). This tumor exhibited anaplastic morphology, suggesting that additional molecular alterations may be required for sarcomatoid transformation and biologic progression.

In the present study, all STs with hotspot MAPK GTPase mutations (*BRAF*, *HRAS*, *NRAS*) were indolent and exhibited diploid genomes, with only one exception (case 7). The latter was clinically indolent but had genomic findings consistent with a shift in ploidy and evidence of a concurrent i(12p). Of note, GCNIS was identified adjacent to this tumor. However, macrodissection and downstream profiling of the ST component demonstrated molecular findings otherwise consistent with the remaining STs. Of note, gains of part or the entirety of chromosome 9 were present in all cases with GTPase mutations, suggesting that both events are required for oncogenesis.

The results of this study seem to indicate that there are (at least) two broad genomic subtypes of STs: one characterized by hotspot mutations of MAPK pathway GTPases and largely diploid genomes and another characterized by a global shift in ploidy and an absence of recurrent pathogenic mutations (on large panel NGS) (Figure 5). In this series, tumors with hotspot *BRAF*/*KRAS*/*NRAS* alterations were always clinically indolent. Malignant cases demonstrated a global ploidy shift with additional recurrent alterations. More specifically, the subset with sarcomatoid transformation consistently harbored pathogenic *TP53* variants. Moreover, another subset of malignant cases (with or without sarcomatoid features) harbored relative gains of 12p, including tumors with evidence of i(12p) by FISH. Interestingly, unsupervised clustering based on genomic methylation profiles showed that two selected samples with gains of 12p (case 2: sarcomatoid ST; case 5: anaplastic ST) clustered closer to typical seminomas than to anaplastic and conventional STs without gains of 12p. This finding suggests that STs with gains of 12p and/or i(12p) may exhibit biologic features akin to those of seminoma [1,5]. Prior studies have shown that STs typically comprise subpopulations of tumor cells with different methylation statuses, suggesting that the separate clustering of seminomas and STs seen in this study could be due to the heterogeneity of the latter [31]. However, most of the samples analyzed herein (12/16) were either sarcomatoid or anaplastic, comprising relatively homogeneous populations of tumor cells compared with conventional STs. Moreover, ascribing the genomic methylation differences between STs and seminomas to the intratumoral heterogeneity of the former fails to explain why malignant STs clustered with seminomas.

This study has limitations that need to be mentioned briefly. First, the number of malignant cases analyzed was limited, which is somewhat unavoidable given that aggressive STs are rare. Second, large panel NGS (rather than whole genome sequencing) was used for the analysis of these samples, limiting the detection of genomic alterations to those present in known cancer-related genes. Third, the work-up of the cases was heterogeneous due to the limited availability of archival material. Despite these shortcomings, the present study yielded informative results that further clarify the molecular events associated with oncogenesis and biologic progression in STs.

In conclusion, our results suggest that there are two subsets of STs with distinct molecular and clinical features. One of them comprises clinically indolent tumors without ploidy shift and *RAS*/*RAF* alterations, whereas the other comprises clinically aggressive neoplasms with i(12p) and/or TP53 alterations. Importantly, relative gains of chromosome 9 represent a recurrent event consistently identified in both subgroups. The identification of +12p/i(12p) in aggressive STs suggests that there are rare testicular germ cell tumors that defy the current developmental classification and may have biological features akin to those of GCNIS-derived germ cell tumors. If the appropriate tests are available in the laboratory, assessment of STs for *TP53* and 12p alterations could be beneficial, especially when the tumors exhibit histopathologic features that have been associated with aggressive clinical behavior (e.g. sarcomatoid or anaplastic histology). The presence of i(12p) and/or pathogenic *TP53* variants in a primary ST probably warrants close clinical follow-up in patients with no evidence of extratesticular disease.

Acknowledgements

This study was carried out with intradepartmental funds from the Department of Pathology of Brigham and Women's Hospital and Mayo Clinic. DM Berney receives support from the Orchid charity for male cancer (UK).

Author contributions statement

SG and AMA designed, coordinated and directed the study. SG, AMA, AOO, JBG, KMC, KM, FM, ED, WJA, JCC, MC, CR, TMU and DMB contributed cases/material. SG, AMA, LMS, YY, MS and RAR analyzed molecular data and interpretated molecular results. SG and AMA drafted the manuscript. All authors made manuscript edits and intellectual contributions. The final version of this manuscript was approved by all the authors.

Data availability statement

The data that support the findings of this study are available from the corresponding author upon reasonable request.

References

1. Oosterhuis JW, Looijenga LHJ. Human germ cell tumours from a developmental perspective. *Nat Rev Cancer* 2019; **19:** 522–537.
2. Giannoulatou E, Maher GJ, Ding Z, *et al*. Whole-genome sequencing of spermatocytic tumors provides insights into the mutational processes operating in the male germline. *PLoS One* 2017; **12:** e0178169.
3. Grogg JB, Schneider K, Bode P-K, *et al*. A systematic review of treatment outcomes in localised and metastatic spermatocytic tumors of the testis. *J Cancer Res Clin Oncol* 2019; **145:** 3037–3045.
4. Mikuz G, Böhm GW, Behrend M, *et al*. Therapy-resistant metastasizing anaplastic spermatocytic seminoma: a cytogenetic hybrid: a case report. *Anal Quant Cytopathol Histopathol* 2014; **36:** 177–182.
5. Gupta S, Farooq A, Rowsey RA, *et al*. Cytogenetics of spermatocytic tumors with a discussion of gain of chromosome 12p in anaplastic variants. *Hum Pathol* 2022; **124:** 85–95.
6. Hu R, Ulbright TM, Young RH. Spermatocytic seminoma: a report of 85 cases emphasizing its morphologic spectrum including some aspects not widely known. *Am J Surg Pathol* 2019; **43:** 1–11.
7. Stueck AE, Grantmyre JE, Wood LA, *et al*. Spermatocytic tumor with sarcoma: a rare testicular neoplasm. *Int J Surg Pathol* 2017; **25:** 559–562.
8. Dias AF, Dvindenko E, Santos F, *et al*. Sarcomatoid spermatocytic tumour: report of a rare case and literature review. *Int J Surg Pathol* 2023; **31:** 728–733.
9. Wagner T, Grantham M, Berney D. Metastatic spermatocytic tumour with hybrid genetics: breaking the rules in germ cell tumours. *Pathology* 2018; **50:** 562–565.
10. Garcia EP, Minkovsky A, Jia Y, *et al*. Validation of OncoPanel: a targeted next-generation sequencing assay for the detection of somatic variants in cancer. *Arch Pathol Lab Med* 2017; **141:** 751–758.
11. Sholl LM, Do K, Shivdasani P, *et al*. Institutional implementation of clinical tumor profiling on an unselected cancer population. *JCI Insight* 2016; **1:** e87062.
12. Abo RP, Ducar M, Garcia EP, *et al*. BreaKmer: detection of structural variation in targeted massively parallel sequencing data using kmers. *Nucleic Acids Res* 2015; **43:** e19.
13. Papke DJ, Nowak JA, Yurgelun MB, *et al*. Validation of a targeted next-generation sequencing approach to detect mismatch repair deficiency in colorectal adenocarcinoma. *Mod Pathol* 2018; **31:** 1882–1890.
14. Christakis AG, Papke DJ, Nowak JA, *et al*. Targeted cancer next-generation sequencing as a primary screening tool for microsatellite instability and lynch syndrome in upper gastrointestinal tract cancers. *Cancer Epidemiol Biomarkers Prev* 2019; **28:** 1246–1251.
15. McCarthy MR, Nichols PE, Sharma V, *et al*. Molecular and immunophenotypic correlates of metastatic epithelioid angiomyolipoma include alterations of TP53, RB1, and ATRX. *Arch Pathol Lab Med* 2023; **147:** 817–825.
16. Gupta S, Erickson LA, Lohse CM, *et al*. Assessment of risk of hereditary predisposition in patients with melanoma and/or mesothelioma and renal neoplasia. *JAMA Netw Open* 2021; **4:** e2132615.
17. Wang Y, Cottman M, Schiffman JD. Molecular inversion probes: a novel microarray technology and its application in cancer research. *Cancer Genet* 2012; **205:** 341–355.
18. Freitag CE, Sukov WR, Bryce AH, *et al*. Assessment of isochromosome 12p and 12p abnormalities in germ cell tumors using fluorescence in situ hybridization, single-nucleotide polymorphism arrays, and next-generation sequencing/mate-pair sequencing. *Hum Pathol* 2021; **112:** 20–34.
19. Gupta S, Sukov WR, Vanderbilt CM, *et al*. A contemporary guide to chromosomal copy number profiling in the diagnosis of renal cell carcinoma. *Urol Oncol* 2022; **40:** 512–524.
20. Serrano J, Snuderl M. Whole genome DNA methylation analysis of human glioblastoma using Illumina BeadArrays. *Methods Mol Biol* 2018; **1741:** 31–51.
21. Aryee MJ, Jaffe AE, Corrada-Bravo H, *et al*. Minfi: a flexible and comprehensive bioconductor package for the analysis of Infinium DNA methylation microarrays. *Bioinformatics* 2014; **30:** 1363–1369.
22. Gu Z, Eils R, Schlesner M. Complex heatmaps reveal patterns and correlations in multidimensional genomic data. *Bioinformatics* 2016; **32:** 2847–2849.
23. Maher GJ, Goriely A, Wilkie AOM. Cellular evidence for selfish spermatogonial selection in aged human testes. *Andrology* 2014; **2:** 304–314.
24. Rahbari R, Wuster A, Lindsay SJ, *et al*. Timing, rates and spectra of human germline mutation. *Nat Genet* 2016; **48:** 126–133.
25. Rosenberg C, Mostert MC, Schut TB, *et al*. Chromosomal constitution of human spermatocytic seminomas: comparative genomic hybridization supported by conventional and interphase cytogenetics. *Genes Chromosomes Cancer* 1998; **23:** 286–291.
26. Looijenga LHJ, Hersmus R, Gillis AJM, *et al*. Genomic and expression profiling of human spermatocytic seminomas: primary spermatocyte as tumorigenic precursor and DMRT1 as candidate chromosome 9 gene. *Cancer Res* 2006; **66:** 290–302.
27. Verdorfer I, Rogatsch H, Tzankov A, *et al*. Molecular cytogenetic analysis of human spermatocytic seminomas. *J Pathol* 2004; **204:** 277–281.
28. Zhang T, Oatley J, Bardwell VJ, *et al*. DMRT1 is required for mouse spermatogonial stem cell maintenance and replenishment. *PLoS Genet* 2016; **12:** e1006293.
29. Matson CK, Murphy MW, Griswold MD, *et al*. The mammalian doublesex homolog DMRT1 is a transcriptional gatekeeper that controls the mitosis versus meiosis decision in male germ cells. *Dev Cell* 2010; **19:** 612–624.
30. Rijlaarsdam MA, Tax DMJ, Gillis AJM, *et al*. Genome wide DNA methylation profiles provide clues to the origin and pathogenesis of germ cell tumors. *PLoS One* 2015; **10:** e0122146.
31. Kristensen DG, Mlynarska O, Nielsen JE, *et al*. Heterogeneity of chromatin modifications in testicular spermatocytic seminoma point toward an epigenetically unstable phenotype. *Cancer Genet* 2012; **205:** 425–431.

SUPPLEMENTARY MATERIAL ONLINE

Figure S1. Conventional ST associated with GCNIS

Figure S2. FSIH in case 5 demonstrated the presence of two *PKP2* signals (red) spatially adjacent to the centromeric probe (green)

Appendix S1. OncoPanel test, genomic coverage

Appendix S2. Genes interrogated by the MayoComplete Solid Tumor Panel